Raman signatures of charge ordering in $K_{0.3}WO_3$

D. M. Sagar,[1,*] D. Fausti,[1] S. van Smaalen,[2] and P. H. M. van Loosdrecht[1]
[1]*Zernike Institute for Advanced Materials, University of Groningen, 9747 AG Groningen, The Netherlands*
[2]*Laboratory of Crystallography, University of Bayreuth, 95440 Bayreuth, Germany*
(Received 5 August 2009; revised manuscript received 16 November 2009; published 28 January 2010)

We present polarization- and temperature-dependent Raman spectroscopic study of hexagonal tungsten bronze, $K_{0.3}WO_3$. The observed asymmetry in phonon line shapes indicate the presence of strong lattice anharmonicity arising due to the nonstoichiometry of the material. We observed a broad multipeak Raman feature at low frequency due to the local modes of K atoms known as local structural excitations. The observed vibrational features indicate a second-order phase transition around $T=200$ K accompanied by a frequency softening of low-frequency phonon modes. The observed phonon anomalies hint a physical picture involving a continuous symmetry change toward a charge-ordered state below 200 K. These observations indicate that $K_{0.3}WO_3$ may exhibit a weak charge-density-wave ground state at low temperatures.

DOI: 10.1103/PhysRevB.81.045124 PACS number(s): 71.45.Lr, 71.30.+h, 78.30.−j

I. INTRODUCTION

Transition-metal oxides exhibit interesting unusual physical properties and have been a subject of intense research. These physical properties often originate from a strong coupling between various elementary excitations in solids, such as phonons, phasons,[1] amplitudons,[2] and plasmarons.[3]

Among the transition-metal oxides, tungsten bronzes have attained considerable attention due to their interesting physical properties which depend on the kind of alkali-metal atom and its composition. Tungsten bronzes are nonstoichiometric compounds with the general formula M_xWO_3 $(0<x<1)$, where M is either an alkali-metal atom or a transition-metal atom (K, Rb, and Tl). These materials undergo one or more structural phase transitions depending on the alkali composition, x.[4,5] Compounds with high x values show high symmetry and compounds with low x values show low symmetry at room temperature.[6] The primary interest in these materials is due to their composition-dependent resistivity anomaly,[5] whose functional form resembles that of charge-density-wave (CDW) systems.[7] The temperature (T_B) at which this resistivity anomaly occurs depends on both the composition and the kind of metal atom as well. It has been established that the resistivity anomaly is associated with a structural transition (T_S) which is due to the ordering of the metal atoms.

Tungsten bronzes with $M=$K, Rb, or Tl exhibit hexagonal symmetry. The hexagonal tungsten bronzes (HTB) have corner-linked octahedra of WO_6 forming a cagelike structure and the metal atoms are positioned at the center of the cage.[8] The structure is stabilized if the metal atoms are large enough to fit into the octahedral cage along the c axis. When the M atoms are small (K, Li, Na) their mobility is remarkably high and this particular nature of tungsten bronzes is responsible for the vast variety of interesting physical properties including the resistivity anomaly,[5,9] observed in these materials. The loosely bound metal atoms along the c axis can give rise to interesting temperature-dependent lattice dynamics due to which one can "move" the metal atoms along the hexagonal c axis using very little thermal energy. The octahedral host cage can further rearrange itself according to a given metal-atom occupancy. Thus, one would expect temperature-dependent rich structural dynamics involving one or more phase transitions.

Further, these materials exhibit interesting physical properties pertaining to their electronic degree of freedom also. Particularly, certain fascinating physical phenomena such as metal-to-insulator transition, lattice ordering, and occurrence of superconductivity can be tuned by continuously varying the doping level, x of the M metal atoms. Further, the metal atoms donate their extra electron(s) to the host cage and are responsible for the conducting properties of these bronzes. Thus, by varying the composition of the metal atoms one can control the conducting properties of these bronzes and the temperature at which the ordering of these metal atoms takes place as well. As evidenced in the neutron-scattering study by Sato *et al.*, the hexagonal tungsten bronzes exhibit two structural phase transitions. The first transition that occurs well below room temperature is associated with the ordering of the metal atoms, hereafter referred to as order-disorder transition. The second phase transition occurs near room temperature which was believed to be due to the distortion of the octahedra. The composition-dependent phase transition was found to be associated with the ordering of the metal atoms (K, Rb, and Tl). The ordering of metal atoms in the octahedral host cage induces a metal-to-insulator transition. Thus the metal-to-insulator transition is associated with a structural phase transition.[4,5]

From x-ray diffraction measurements it is known that the ordering of the metal atoms is associated with a doubling of the unit cell at low temperatures.[5] Thus for low temperatures a complete ordering of the metal atoms is possible only for the optimal doping, $x=0.25$, since this corresponds to a full occupation of two atoms per unit cell.[10] On the other hand, in the over-doped case, $x=0.33$, the metal atoms completely fill the hexagonal cage at room temperature. Intuitively one would not expect any temperature-dependent metal-atom ordering for $x=0.33$. For all other compositions the ordering is expected to be partial and incomplete. Thus, an incomplete order-disorder transition would lead to physical properties that are strongly depending on the composition and ionic radius of the metal atom.[11] Resistivity measurements and neutron-scattering measurements have indicated that the

above-mentioned resistivity anomaly (T_B) corresponds to the structural phase transition as they both occur at the same temperature for a given x value, thus explaining the observed resistivity anomaly in these materials. These materials have been explored experimentally focusing on their electronic resistivity and lattice ordering by Cadwell[5] and Sato.[4] Recently, Rb counter parts of the materials were extensively investigated by Brusetti *et al.*[9,11,12] focusing primarily on their superconducting properties. For $x=0.25$, the recent angle-resolved photoemission studies revealed the existence of a hidden one-dimensional (1D) Fermi surface (FS) nesting showing the possibility of a charge-density-wave ground state.[13] A detailed study of soft-lattice modes in metallic Na_xWO_3 has been reported by Flynn.[14]

However, experimental studies focusing upon the lattice dynamics are limited to the previous neutron studies by Sato *et al.* Optical spectroscopic properties of these materials remain still unexplored.

On a general note, optical spectroscopic experiments are capable of revealing the presence of phase transitions,[1] charge ordering,[15] and the presence of novel ground state such as arising due to electron-phonon coupling.[2] One main advantage of polarized Raman scattering technique over neutron is that the former can access anisotropic properties (Raman selection rules) of low-frequency phonon modes related to "long-wavelength" lattice degrees of freedom and optical phonons ($k\sim 0$) as well.

In this paper we present a polarization- and temperature-dependent Raman study of $K_{0.3}WO_3$. As expected, the observed Raman features exhibit strong disorder in this material. We observed signatures of a second-order phase transition at $T=200$ K. We also observed optical phonon softening as initially predicted by Sato *et al.*[4] The Raman spectra are strongly polarized in the (cc) direction. We discuss the Raman features in terms of frequency and linewidth. We observed multipeak Raman features which we ascribe to a strong anharmonicity driven by lattice disorder. Further, many hitherto existing experimental evidences, including the present one, strongly suggest that some kind of charge ordering taking place in $K_{0.3}WO_3$ and further hints the possibility of a "dirty charge-density-wave" ground state below $T=200$ K.

II. EXPERIMENTAL

The tungsten bronzes with M_xWO_3 (M=K,Rb) were reported to exhibit hexagonal crystal structure at room temperature with space group $P6_3/mcm(D_{6h}^3)$ as suggested by Magneli.[8,12] A recent study by Brusetti *et al.*,[12] on $Rb_{0.3}WO_3$ compounds suggests the possibility of an orthorhombic distortion of the hexagonal lattice at low temperatures. The analysis of the Raman spectra in the present study is in line with the established hexagonal symmetry. In the present study, the orientation of the sample was achieved by performing x-ray diffraction measurements.

Single-crystalline material of $K_{0.3}WO_3$ was prepared by the temperature-gradient flux method as described in Ref. 16. After surface polishing, samples were mounted in an optical flow cryostat (temperature stabilization better than 0.1 K) and backscattering Raman spectra were recorded (frequency resolution ~ 2 cm^{-1}) using a triple grating monochromator in subtractive mode equipped with a liquid-nitrogen cooled CCD detector. A solid-state diode-pumped, frequency-doubled Nd:YVO_4 laser system is used as excitation source (wavelength 532 nm, spot size 10 μm). The power density was kept below 100 W/cm^2 in order to minimize heating effects. The polarization was controlled on both the incoming and outgoing beams, giving access to all the polarizations allowed by the backscattering configuration. The measurements were done for both the incident and scattered light being parallel to the hexagonal axis, referred to as (cc) and both perpendicular to the hexagonal axis (aa). The cross-polarization spectra did not yield appreciable scattering intensity and will therefore not be discussed here.

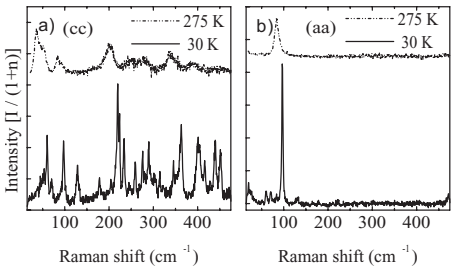

FIG. 1. Raman spectra at 275 and 30 K for (cc) configuration in panel (a) and for (aa) in panel (b). The spectra are normalized by their respective Boltzman factors, $1/[1+n]$, where $n(\omega,T)=1/(1+e^{(\hbar\omega/k_bT)})$.

III. RAMAN SPECTRA AT T=275 AND 30 K

Figure 1 shows the Raman spectra of $K_{0.3}WO_3$ at $T=275$ and 30 K for (cc) [panel (a)] and (aa) [panel (b)] polarizations. The spectra are normalized to their respective Boltzman factors, $[1+n]$, where n is the temperature- and frequency-dependent phonon occupation number. Along the hexagonal axis or (cc) at $T=275$ K there are five strong modes whose frequencies are 35, 50, 83, 201, and 337 cm^{-1}. The phonon modes at 157, 247, 278, and 383 cm^{-1} are very broad and weak. Thus the room-temperature Raman spectrum of $K_{0.3}WO_3$ shows rich Raman features in contrast to the previous study by Scott *et al.*,[17] where no Raman lines were observed for the hexagonal $Rb_{0.3}WO_3$.

In (aa) configuration [Fig. 1(b)] there is only one strong phonon mode at 83 cm^{-1} at $T=275$ K, but there are few weaker modes as well. The phonon modes with frequencies <200 cm^{-1} are due to W-O-W bending modes and those which are <450 cm^{-1} are the bending modes due to O-W-O vibrations. The stretching modes due to W-O vibrations usually appear at higher frequencies. These assignments are a general feature of any transitional-metal compounds forming octahedral coordinates and are corroborated with the previous studies.[18,19] One may notice the absence of any sharp Raman lines or in other words, the broad over-damped vibrations [for instance, in (cc)] reflect either the presence of vacancies and/or presence of strong electron-phonon coupling. As mentioned earlier, the M_xWO_3 bronzes are dominated by

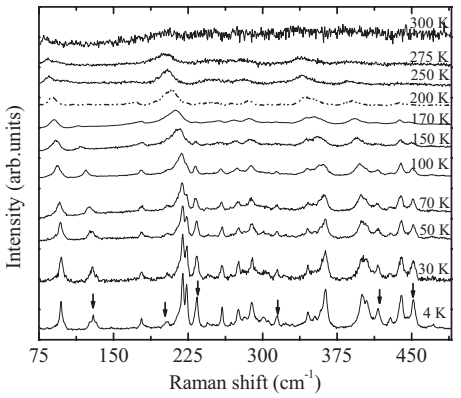

FIG. 2. Temperature-dependent Raman spectra of $K_{0.3}WO_3$ in (cc). The spectra are vertically shifted for clarity. The modes indicated by arrows tend to vanish around $T=200$ K, indicating a second-order transition.

lattice disorder arising primarily due to the vacancies on the alkali-atom sublattice. The asymmetric line shapes of the Raman lines in Fig. 1 hint the role lattice anharmonicity arising mostly due to K sublattice disorder. This interpretation gains weight when one examines the phonon line shapes for (aa) polarization. The line shapes are perfectly Lorentzian (right panel, Fig. 1) for both the temperatures. In other words, the (cc) configuration spectra reveal the superlattice ordering.

The Raman spectra for (aa) and (cc) at $T=30$ K shows many new Raman vibrational features. As the Raman spectrum in (cc) configuration is richer in Raman features, we restrict our discussion to mainly on this particular polarization configuration. The appearance of many new modes at low temperature hints toward the possibility of a temperature-dependent phase transition. We carried out a detailed temperature-dependent study for both polarizations.

IV. TEMPERATURE-DEPENDENT RAMAN SPECTRA

The temperature-dependent Raman spectra for (cc) are shown in Fig. 2. For very low temperatures ($T<100$ K) one can notice many sharp Raman features indicating a stable or ordered phase. The asymmetric line shape of these phonon modes also imply the role of lattice disorder in these materials. The modes marked by arrows in the low-temperature spectrum undergo frequency softening and line-width broadening as the temperature is increased and they tend to vanish at $T=200$ K, indicating the possible occurrence of a second-order phase transition. The line shapes in the low-temperature spectrum (4.2K) are non-Lorentzian. Non-Lorentzian line shapes would immediately imply strong lattice anharmonicities involved in the scattering process. The lattice anharmonicity typically arises due to higher order scattering processes,[20] Fano-type line shapes resulting from the interaction of a single state with a continuum of states[21] or breakdown of wave-vector conservation due to disorder.[22,23] It has been shown in the case of ferroelectric material $PbTiO_3$ that non-Lorentzian line shapes can also arise from a first-order Raman scattering process exhibiting multiple subpeaks in "a single phonon" Raman line.[22] The case of Fano type of process may be unlikely since the line shapes for higher temperatures do not support this picture. However, a temperature-dependent progression of Fano interference cannot be discarded completely.[24] As can be seen in the next section, a significant enhancement of the integrated intensity of the low-frequency modes for higher temperatures compel us to ascribe the observed non-Lorentzian line shape as arising due to a disorder-induced breakdown of wave-vector conservation. Further, this claim is supported by the presence of a failed perfect order-disorder transition arising due to the nonstoichiometry of $K_{0.3}WO_3$.

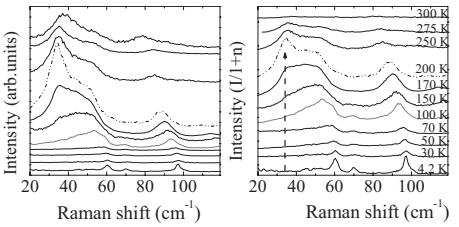

FIG. 3. Temperature-dependent low-frequency Raman spectra of $K_{0.3}WO_3$ in (cc). Left panel shows the unscaled Raman spectra and the right panel shows the Raman spectra divided by their respective Boltzman factors, $1/[1+n]$, where $n(\omega,T)=1/(1+e^{(\hbar\omega/k_BT)})$. The dashed vertical arrow indicates new mode coming up at 35 cm^{-1} between $T=70$ and 100 K.

Thus, the temperature-dependent Raman spectra along (cc) exhibit signatures of a second-order phase transition near $T=200$ K together with non-Lorentzian line shapes that are ascribed to inelastic light scattering of lattice disorder in this nonstoichiometric material.

A. Low-frequency modes

Figure 3 gives the temperature-dependent Raman spectra of $K_{0.3}WO_3$ for (cc) in the frequency region 20–100 cm^{-1}. From the right panel it is clear that the low-frequency Raman features show very strong temperature-dependent behavior with respect to their frequency, linewidth, and scattering intensity. At $T=4.2$ K, there are distinctly five Raman lines at 45, 50, 60, 70, and 97 cm^{-1}. The modes at 45 and 60 cm^{-1} are also seen in the neutron study of $Tl_{0.33}WO_3$ but not in the parent compound WO_3.[25] Therefore, these modes are interpreted as arising due to the local modes of the alkali atoms. In the Tl compound these modes were found at slightly lower energies; 20 and 43 cm^{-1} and were ascribed to the dispersionless Einstein-type phonon branches arising due to the local movement of Tl atoms. In contrast to the previous neutron-scattering studies where the features were seen as broad, in the present Raman study the modes are well resolved. Recalling the study of Rb_xWO_3 by Sato *et al.*,[4] a very broad feature of about 40 cm^{-1} width with central frequencies 44 and 48 cm^{-1} was observed at $T=35$ K and it gained strength at higher temperatures. These features were assigned to the dispersionless Einstein-type modes due to the local vibration of the Rb atoms. The HTB bronzes typically form cagelike structure by the corner-linked octahedra (WO_3) surrounding the alkali (or K, Rb) atoms. Due to this structural

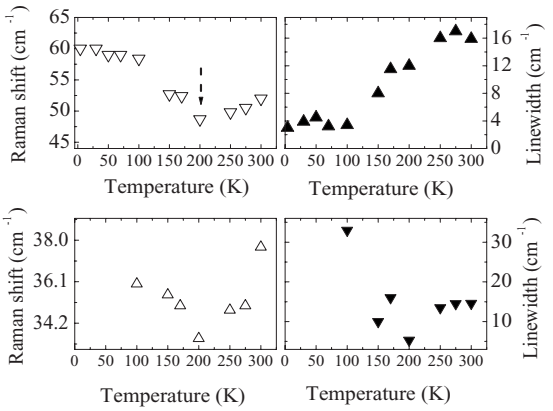

FIG. 4. Temperature-dependent frequency and linewidth of 60 and 35 cm^{-1} phonon modes. The vertical arrow indicates the temperature above which the frequency of the modes start to harden slightly.

configuration the K atoms are loosely bound to the octahedral tunnels and lead to local structural modes seen in the low-frequency part of the Raman spectrum. In line with the previous studies, we ascribe the low-frequency band as arising mostly due to the local movements of loosely bound K sublattice. As the temperature is increased the mode at 60 cm^{-1} gains strength and undergoes frequency softening. Above $T=100$ K a new mode appears at 35 cm^{-1} and grows until $T=250$ K, as indicated by the broken vertical arrow in the right panel, Fig. 3. Both these modes show frequency hardening (by ~ 2 cm^{-1}) between $T=200$ and 300 K. A weak mode at 70 cm^{-1} vanish above $T\sim 200$ K.

Figure 4 presents the temperature-dependent behavior of the low-frequency Raman lines, 35 and 60 cm of $K_{0.3}WO_3$ in (cc) configuration. Until $T=100$ K the frequency and the linewidth of 60 cm^{-1} phonon mode shows no change. The frequency softening occurs between $T=100$ and 200 K. Above $T=200$ K, it shows slightly hardening behavior and the linewidth almost saturates. Due to the presence of multipeak or subpeak Raman feature the fitting procedure is complicated and hence may not be reliable. Therefore whether there is a slight decrease in the linewidth above 200 K is merely speculative. Obviously, a major change in frequency and linewidth occur between 100 and 200 K.

The phonon mode at 35 cm^{-1} is absent for lower temperatures. Above 100 K, the mode undergoes a systematic frequency softening until $T=200$ K above which it clearly hardens by about 4 cm^{-1} (see Fig. 3 also).

Evidently, the temperature-dependent behavior of 60 cm^{-1} phonon mode typically resembles that of a "soft mode" expected from a second-order phase transition. On the other hand, further hardening above 200 K implies the role of lattice anharmonicity which may originate from a rearrangement of the K sublattice. In other words, the "frequency switching" (from softening to hardening) behavior may hint the presence of a different phase above 200 K.

We further analyze the low-frequency A_g Raman band by fitting with three Lorentzians as shown in Fig. 5. The fits are mostly indistinguishable from the experimental data. The temperature-dependent fits reveal three distinct Raman features whose frequencies are very weakly temperature dependent in the temperature range 150–200 K. However, the striking feature is the relative intensity of 35 and 60 cm^{-1} modes. The mode at 35 cm^{-1} appears only above $T=100$ K. As can be inferred from the fit, the relative intensities of these two phonon modes change with increasing temperature. The interplay of the phonon modes 35 and 60 cm^{-1} with temperature can be seen from Fig. 5. The relative intensity, $R=I(35\ \text{cm}^{-1})/I(60\ \text{cm}^{-1})$ of these modes is plotted in the bottom panel in Fig. 5. A substantial variation in R with respect to temperature clearly shows that the high-temperature phase is different than the low-temperature one.

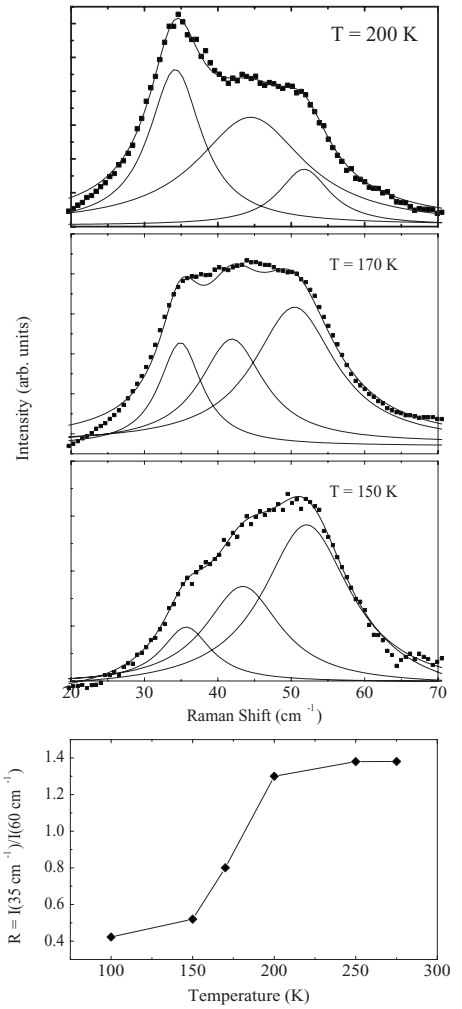

FIG. 5. The top three panels show temperature dependence of the line shape of low-frequency A_g band. The symbols represent experimental data and solid lines represent fit to a sum of Lorentzian functions. The relative intensities of 35 and 60 cm^{-1} phonon modes reverse order with temperature. The bottom panel shows the temperature-dependent intensity ratio, R, of 35 and 60 cm^{-1} modes. See text for details.

All these observations are commensurate with the following physical picture. At very low temperature, say $T=4.2$ K, the K sublattice is in a frozen-in state due to which it shows the five weak but distinct modes. As the temperature is increased the K sublattice starts to randomize their occupancies giving rise to a strongly disordered metastable state. Due to this disorder the wave-vector conservation rules for

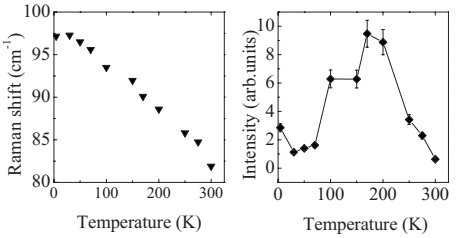

FIG. 6. Left panel: the temperature-dependent frequency (left panel) and the anomalous integrated intensity (right panel) of 97 cm^{-1}.

Raman scattering are relaxed resulting in intensity-enhanced Raman features. Further, the interplay of the modes at 35 and 60 cm^{-1} implies two distinct structural phases, as in the case of σ-AgI.[26]

A structural phase transition found in the neutron-scattering study by Sato *et al.* were interpreted as arising due to the ordering of the alkali atoms. For the composition $x=0.25$ this order-disorder transition is of first-order kind of transition and is complete. This is justified by the physical scenario where the ordering of local alkali atoms is accompanied by the doubling of the unit cell. For $x=0.25$, the doubling of unit cell would corresponds to one alkali atom per unit cell thus making the ordering complete. For compositions other than $x=0.25$ the complete ordering accompanied by the doubling of the unit cell is counter intuitive. In the present case where $x=0.3$, the disorder in the K sublattice is reflected in the strongly temperature-dependent low-frequency modes. The hardening of the modes above $T=200$ K and the decreasing linewidths are due to an incomplete-ordered state of the K sublattice. The structural phase stabilizes further as the temperature is increased. It is worth mentioning that the order-disorder temperature (T_S) also corresponds to the strong resistivity anomaly observed in these materials.[5]

Further evidence of the order-disorder kind of transition may be observed by referring to Fig. 6. The integrated intensity of 97 cm^{-1} mode shows an anomalous behavior. The integrated intensity of 97 cm^{-1} mode increases with increasing temperature and peaks near 200 K, above which it drops down significantly. Evidently, the signatures of strong temperature-dependent disorder have been observed. A more stable phase seems to evolve near the room temperature and above.

B. Octahedral modes

Figure 7 shows the temperature dependence of few selected octahedral phonon modes in (cc). From the top panel it can be seen that the phonon line shapes are clearly non-Lorentzian at low temperatures, however, they tend to become more symmetrical as the temperature approaches room temperature. This observation again hints that the high-T phase is a relatively better ordered phase. By observing the low-temperature Raman spectra one may notice several interesting features, (a) splitting of the octahedral modes below 100 K, (b) frequency softening and line-width broadening between $T=100-200$ K, and (c) saturation of the phonon

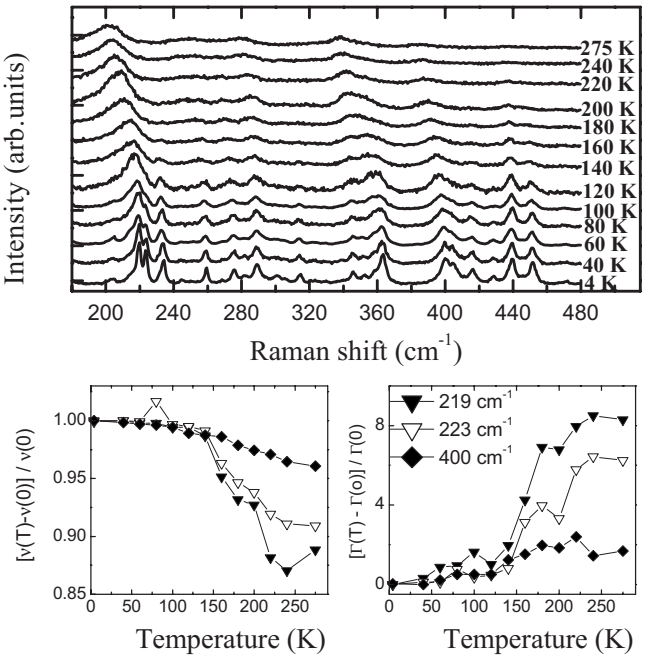

FIG. 7. Top panel: the temperature-dependent Raman spectra of the octahedral modes in (cc) showing the frequency softening (the spectra are vertically shifted for clarity). The temperature-dependent frequency softening and line-width broadening (bottom panels) indicate a second-order phase transition taking place near 200 K.

frequency and the linewidth below 100 K. All these feature indicate that the octahedral modes couple strongly to the observed phase transition. The observation of a larger number of octahedral modes below 100 K would imply that Jahn-Teller (J-T) kind of distortion might be present at low temperature. Further, this claim can be justified due to the presence of a single unpaired electron in the e_g orbital. At low-temperatures one would expect a localization of the unpaired electron which would facilitate the J-T kind of distortion lifting the degeneracy of the orbitals. Above 200 K, the electron is delocalized restoring the degeneracy of the e_g orbitals. This interpretation is commensurate with the fact that the high-T phase is metallic and the low-T phase is an insulating charge-ordered state, which is reported in the literature.

All these features (particularly, the broad phonon modes above 200 K) suggest a scenario involving strong electron-phonon coupling arising primarily due to the thermally activated K-sublattice disorder, which might be absent or weak at low temperatures. The possible occurrence of a second-order phase transition is evidenced by the vanishing of several weak Raman features marked by arrows in Fig. 2 (see also Fig. 7). At present the exact nature of the phase transition remain elusive (*vide infra*).

V. DISCUSSION

When compared to the Na counter part of tungsten bronzes (Na_xWO_3), K_xWO_3 bronzes have attained little attention. Optical spectroscopic studies on these bronzes are

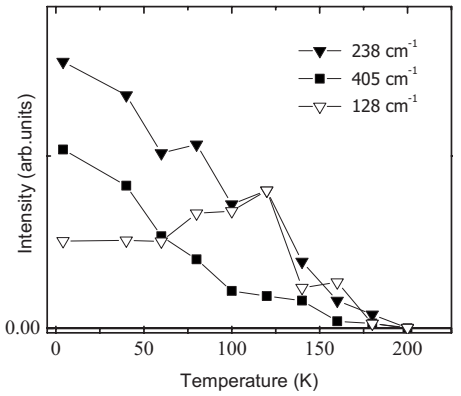

FIG. 8. Temperature-dependent intensities of some phonon modes (as indicated in Fig. 2) showing that the modes vanish around 200 K.

limited. However, recent studies have revisited the interest in these bronzes using angle-resolved photoelectron spectroscopy (ARPES) and revealed many interesting electronic structure related properties.[13] Particularly ARPES on $x=0.25$ samples revealed the presence of a hidden 1D Fermi surface in conjunction with FS nesting, which is typically observed in charge-density-wave materials.[13] The observation of superlattice reflection by powder neutron-diffraction[27] and electron diffraction[10] experiments indeed support the possibility of Fermi-surface nesting accompanied by a CDW formation. The FS nesting in only one particular direction $[\Gamma(M)]$ for $x=0.25$ revealed by ARPES suggests a weak FS instability. This would imply a weak CDW ground state and hence the degree of FS nesting may depend strongly on composition. As mentioned earlier, although the conduction band of $K_{0.3}WO_3$ is comprised of d band of W, the K atoms dope electrons into the conduction band. Thus, one would expect a one-to-one correlation between the composition, x and the observed FS nesting. This would mean a possible presence of "dirty CDW" state for other compositions.

We have a number of reasons to believe the presence of a weak CDW state in $K_{0.3}WO_3$. We observed a temperature-dependent soft-mode behavior of 60 and 220 cm^{-1}, implying a "displacive" nature of the observed phase transition in $K_{0.3}WO_3$. As shown in Figs. 2 and 8 many of the sharp Raman lines that are seen at low temperature vanish around 200 K. These phonons may be nothing but the so-called phase phonons, which typically arise due to the folding of the Brillouin zone below T_C (200 K). Further, the frequency softening of certain phonons (364 and 220 cm^{-1}) and the frequency saturation below 100 K very much resemble the behavior of soft modes, for instance, seen in the prototypical CDW system—blue bronze.[2] The saturation of frequency and linewidth of 220 cm^{-1} mode above 200 K very much implies a strong electron-phonon coupling. In general, phonon line-width broadening may come from either phonon-phonon interaction in which case an optical phonon decays into two acoustic phonon modes, or due to an anharmonicity arising from electron-phonon coupling. If the anharmonicity is of phonon-phonon type one would not expect the linewidth or frequency of the mode to saturate above a certain temperature. The softening should continue for all the temperatures. On the other hand, if it originates from an electron-phonon-interaction mediated phase transition, one would expect the observed frequency saturation above certain temperature, in the present case 200 K.

The octahedral modes are found to couple strongly to the observed phase transition. The frequency softening is as much as 12%. The "steplike" behavior in the linewidth of the octahedral modes above 100 K shows that an additional decay channel becomes available above 100 K. This additional decay channel could very well be that the single unpaired electron which becomes delocalized above 100 K. Below 100 K, we observed a larger number of octahedral modes which is again consistent with the proposed J-T distortion below 100 K. The valence electronic configuration of atomic W is $5d^46s^2$. In the parent compound WO_3 the ionic configuration of W has lost all it's valance electrons. Indeed solid WO_3 is an insulator. Thus the origin of electronic conduction is due to the M atoms which dope electrons into the $5d$ conduction band. Due to the octahedral crystal field the energy associated with the t_{2g} orbitals is lower than the e_g orbitals. Further, due to the hexagonal symmetry the orbitals are further split into the lowest doublets (d_{xz},d_{yz}) and an upper singlet d_{xy}. The doubly degenerate orbital can be subject to Jahn-Teller distortion. A cooperative Jahn-Teller distortion may be expected for sufficiently high doping.

On the other hand, we also find evidences for a strong disorder in $K_{0.3}WO_3$. For instance, the integrated intensity of 97 cm^{-1} enhances until $T=200$ K from below and drops down, implying the role of lattice disorder. Specifically, the enhancement of the Raman intensity is due to a disorder-driven breakdown of wave-vector conservation which leads to enhanced Raman intensity. The observed non-Lorentzian line shapes for low and intermediate temperatures also hint the influence of strong lattice anharmonicity arising due to the lattice disorder. Similar arguments hold good for the low-frequency Raman band (Fig. 3). As expected, we did not find any evidence for a first-order nature (such as sudden appearance of new Raman features or a frequency discontinuity) of order-disorder transition. This observation is in line with the previous predictions by Sato *et al.*, that a perfect K ordering accompanied by a unit cell doubling is possible only for $x=0.25$.

In a CDW ground state one expects to observe the transverse amplitudon mode in Raman experiments. In the present case, such observation might be masked either due to (a) the broad "local-mode" feature associated with temperature-dependent K lattice ordering between 20–100 cm^{-1} or/and (b) without evidences from neutron- and x-ray scattering measurements it is impossible to ascribe any observed mode confidently as *amplitudon*. Further, due to a competition between lattice disorder and electron-phonon-mediated charge ordering, $K_{0.3}WO_3$ may be considered as a "weak/dirty CDW." In other words, in the more perfectly ordered case of $x=0.25$, the CDW signatures may be prevalent.

VI. CONCLUSIONS

In conclusion, we presented temperature-dependent and polarization-resolved Raman spectroscopic study of

$K_{0.3}WO_3$. To the best of our knowledge, this is the first Raman spectroscopic study in M_xWO_3 bronzes reported so far. The Raman features observed are quite complex in nature implying the role of disorder and lattice dynamics. We observed Raman features associated with K lattice ordering and two soft modes at 60 and 220 cm^{-1}. The observed phase transition evidenced by the vanishing of many phonon modes at $T=200$ K could be the "zone-folding" modes. The strong variation in the ratio of intensity of 30 and 60 cm^{-1} phonon modes reveals the interplay between two crystallographically different phases. The octahedral modes are found to couple strongly to the charge ordering, possibly undergoing Jahn-Teller distortion locally below $T\sim 100$ K. Further study on other compositions is necessary to verify the possible presence of CDW ground state in these bronzes. $K_{0.3}WO_3$ may be considered as an example of a dirty CDW compound.

*Present address: Department of Chemistry, University of Durham, Durham, UK; m.s.dodderi@dur.ac.uk

[1] L. Degiorgi, B. Alavi, G. Mihály, and G. Gruner, Phys. Rev. B **44**, 7808 (1991).
[2] D. M. Sagar, D. Fausti, S. Yue, C. A. Kuntscher, S. van Smaalen, and P. H. M. van Loosdrecht, New J. Phys. **10**, 023043 (2008).
[3] R. Tediosi, N. P. Armitage, E. Giannini, and D. van der Marel, Phys. Rev. Lett. **99**, 016406 (2007).
[4] M. Sato, B. H. Grier, H. Fujishita, S. Hoshino, and A. R. Moodenbaugh, J. Phys. C **16**, 5217 (1983).
[5] L. H. Cadwell, R. C. Morris, and W. G. Moulton, Phys. Rev. B **23**, 2219 (1981).
[6] G. Andersson, Acta Chem. Scand. (1947-1973) **7**, 154 (1953).
[7] G. Gruner, Rev. Mod. Phys. **60**, 1129 (1988).
[8] A. Magneli, Nature (London) **169**, 791 (1952).
[9] R. Brusetti, P. Bordet, and J. Marcus, J. Solid State Chem. **172**, 148 (2003).
[10] H. B. Krause, W. G. Moulton, and R. C. Morris, Acta Crystallogr. B: Struct. Sci. **B41**, 11 (1985).
[11] R. Brusetti, P. Haen, and J. Marcus, Phys. Rev. B **65**, 144528 (2002).
[12] R. Brusetti, P. Bordet, J. Bossy, H. Schober, and S. Eibl, Phys. Rev. B **76**, 174511 (2007).
[13] S. Raj, T. Sato, S. Souma, T. Takahashi, D. D. Sarma, P. Mahadevan, J. C. Campuzano, M. Greenblatt, and W. H. McCarroll, Phys. Rev. B **77**, 245120 (2008).
[14] E. J. Flynn, Phys. Rev. B **21**, 1105 (1980).
[15] C. Presura, M. Popinciuc, P. H. M. van Loosdrecht, D. van der Marel, M. Mostovoy, T. Yamauchi, and Y. Ueda, Phys. Rev. Lett. **90**, 026402 (2003).
[16] K. V. Ramanujachary, M. Greenblatt, and W. H. McCarroll, J. Cryst. Growth **70**, 476 (1984).
[17] J. F. Scott, R. F. Leheny, J. P. Remeika, and A. R. Sweedler, Phys. Rev. B **2**, 3883 (1970).
[18] M. Boulova, N. Rosman, P. Bouvier, and G. Lucazeau, J. Phys.: Condens. Matter **14**, 5849 (2002).
[19] M. Maczka, J. Hanuza1, and A. Waśkowska, J. Raman Spectrosc. **34**, 432 (2003).
[20] S. A. Solin and A. K. Ramdas, Phys. Rev. B **1**, 1687 (1970).
[21] U. Fano, Phys. Rev. **124**, 1866 (1961).
[22] C. M. Foster, M. Grimsditch, Z. Li, and V. G. Karpov, Phys. Rev. Lett. **71**, 1258 (1993).
[23] I. K. Marmorkos and S. Das Sarma, Phys. Rev. B **45**, 13396 (1992).
[24] S. Lupi, M. Capizzi, P. Calvani, B. Ruzicka, P. Maselli, P. Dore, and A. Paolone, Phys. Rev. B **57**, 1248 (1998).
[25] W. A. Kamitakahara, K. Scharnberg, and H. R. Shanks, Phys. Rev. Lett. **43**, 1607 (1979).
[26] A. Fontana, G. Mariotto, and M. P. Fontana, Phys. Rev. B **21**, 1102 (1980).
[27] J. Schultz, H. Horiuchi, and H. B. Kause, Acta Crystallogr., Sect. C: Cryst. Struct. Commun. **42**, 641 (1986).